A first-order transition in the charge-induced conformational changes of polymers

Yi Mao, Alexander L. Burin,[a] Mark A. Ratner, and Martin F. Jarrold
Department of Chemistry, Northwestern University, Evanston, Illinois 60208

(Received 12 July 2001; accepted 22 March 2002)

Analytical mean-field theories and lattice model simulations have been used to study the charge-induced conformational changes of single polymer molecules. The compact-to-extended transition induced by charge is found to be first-order (i.e., two-state transition with a transition state) in the presence of strong short-range interactions at low temperatures. Short-range interactions decay much faster than electrostatic energy so expansion below a minimal value cannot produce electrostatic compensation for short-range energy loss. This is the origin of a free energy barrier (transition state) between the compact and the extended states. If the short-range interactions are weak in comparison with attractive and repulsive Coulomb interactions, the transition is expected to be second-order (one-state transition without a transition state). The prediction is compared to the computer simulation of the exhaustive enumeration of all 12-mer cubic lattice polymer conformations using different potentials, and qualitative agreement is found. Implications for protein folding and unfolding are discussed. © *2002 American Institute of Physics.*
[DOI: 10.1063/1.1478771]

I. INTRODUCTION

Electrostatics has long been recognized as one of the major contributions to the free energy of macromolecules. The well-known phenomenon of acid denaturation of proteins clearly demonstrates the *p*H-dependence of protein stability.[1] The instability induced by additional charges occurs to gas-phase proteins[2] and synthetic polymers[3] as well. Despite diversity in materials and medium, a sharp, discontinuous transition in size, measured as a function of charge or pH at low temperatures, is found to be a common feature of this electrostatically driven process. Understanding how electrostatics affects stability has been the subject of theoretical studies for many decades.[4–6] Among all the approaches, the underlying assumption is that electrostatic dipole–dipole interaction is believed to be the primary force controlling charge or *p*H dependent phenomena[7] and often it is the only factor under consideration. Reproduction of the dependence of protein stability upon *p*H is mainly based upon calculation of the sum of pairwise electrostatic interactions of amino acids.[7] Recently, instabilities of charged polyampholytes have been studied by Monte Carlo simulations on lattice models composed of oppositely charged beads and the phase transition[8] from a compact to extended configuration was found when the charge exceeded a threshold value.[9,10]

A delicate balance of all the important interactions, including van der Waals, hydrophobic, hydrogen bond, and electrostatic interactions, as well as entropy, determines the stability of macromolecules. Experiments show that frustrated interactions may cause a discontinuous or continuous phase transition in polymers.[3] Molecular-dynamics simulations also reveal that the energy difference between the compact low charge states and unfolded high charge states of proteins is determined by a balance between Coulomb repulsion, attractive electrostatic interaction and van der Waals interaction.[11–14] Thus in order to understand the underlying physical picture of electrostatically driven conformational changes in polymers, it is necessary to consider the major competitive forces, and not exclusively electrostatics. The competition between opposite forces determines the overall conformation. Obviously, the repulsive charge interaction favors extension of the molecules, and the opposite forces favoring compactness are the attractive Coulomb interaction and van der Waals interaction. The nature of the phase transition driven by electrostatics is poorly understood, that is, what the dominant forces are and especially how they relate to the order of phase transitions have not been fully clarified.

The goal of this paper is to investigate the nature of phase transitions and address the bonding and interaction properties that govern the stability of polymers. We use analytical arguments based on Flory's mean-field theory[15] for the homopolymer and lattice model simulations to address these issues. Following this model[15] we do not consider the details of the short-range coupling of nearby monomers in the polymer chain. Although this interaction can strongly affect the nature of the folding collapse transition in short polymers (see, e.g., Ref. 16), we believe that a simple random walk picture can be applied, when the polymer size is much larger than its persistence length. These effects are included into the entropy definition for the coarse-grained random walk model, while the energetics is defined entirely by the interactions of monomers located far from each other in the polymer chain. For these interactions one can separate the long-range Coulomb interaction of external charges and the short-range interactions including van der Waals, dipolar, hydrophobic, etc. forces, which decreases with distance very quickly. The latter are significant for the closely located

[a]Electronic mail: a-burin@nwu.edu

TABLE I. Definition of radii used through the paper.

Notation	Dependence on N	Definition
l_0	$l_0 \propto N^0$	Size of the monomer
$R_{\min}$	$R_{\min} \sim l_0 N^{1/3}$	Minimum gyration radius of the folded state
$R_{\max}$	$R_{\max} \sim l_0 N$	Maximum gyration radius of the aligned (highly charged) state
R_0	$R_0 = l_0 N^{1/2}$	Random walk length from the beginning to the end of the polymer chain
R_∞	$R_\infty \approx \frac{1}{2^{1/5}} N^{3/5} (l_0^2 v_0)^{1/5} \propto l_0 N^{3/5}$	Characteristic gyration radius of the long polymer at high temperature
R_{ext}	$R_{\text{ext}} = R_0 \left(\frac{\eta Q^2}{\epsilon R_0 3 k_B T} \right)^{1/3}$	Gyration radius in unfolded state of highly charged polymer with short range interaction
R_m	$R_m \approx R_{\min} \left(\frac{3E_{\text{sh}}}{E_C} \right)^{1/3}$.	Gyration radius for the free energy maximum

monomers only. The folding–unfolding transitions are caused by the competition between the long-range and short-range forces, defined above.

The paper is organized as follows: We begin with an analytic treatment and then compare those results with the computer simulations. In Sec. II the model for the polymer charging and the analytical expression for the free energy are obtained in two different regimes of short-range and long-range interaction of different monomers. In Sec. III we apply this model to study the folding and unfolding caused by the external charging of a polymer composed by monomers with the short-range interaction (Sec. III A) or charged monomers with the long-range Coulomb interaction (Sec. III B). The system of charged monomers shows a qualitatively different transition between compact and extended state. Therefore this system is interesting as the alternative to discontinuous change of the molecular size with charging in the case of the short-range interaction. In Sec. IV a lattice model simulation is completed to study the validity of analytical theory and analyze the limiting cases where the mean-field description fails. In Sec. V the comparison of different approaches with each other and experimental data is presented.

II. MODEL AND FREE ENERGY

For the sake of simplicity we use the model for the homogeneous polymer, suggested by Bryngelson and Wolynes.[15] Certainly this model does not have all the ingredients for understanding the phase transition of heterogeneous polymers, but it gives a reasonable description for the size of the molecule as a function of temperature and charge at sufficiently low temperatures. The energy minima and the energy barrier between them are derived, and their physical meanings are discussed.

Consider a coarse-grained random walk model. The conformation of an ideal chain composed of N monomers can be represented as a random walk of N steps from the origin to some end point R. R gives the typical size of the system, i.e., the radius of gyration of the chain to a crude approximation, it can also be defined as the mean-square deviation of monomer coordinates from the center of the system. (More generally the elementary step contains a finite number of monomers since the angle between two neighbor monomers cannot be too large. This is not important for our results although it can affect the quantitative applications.)

The gyration radius R characterizes the scattering cross section for gas-phase experiments,[2,12] where the charged polymer molecules move in an applied electric field. The scattering process arises from collisions of the polymers with inert gas host atoms. When the polymer is in the compact (folded) state its scattering cross section is given by the squared gyration radius

$$\sigma \sim R^2, \tag{2.1}$$

since the polymer molecule is not transparent to the gas molecules. When the gyration radius exceeds some critical value R_c where the molecule becomes partially transparent and the scattering cross section increases much slower than predicted by Eq. (2.1). However the scattering cross section should always increase with the gyration radius and we expect that the transition from the folded state to the unfolded state caused by the addition of charge should be accompanied by a remarkable change of the scattering cross section. This change can be either continuous for continuous change of the gyration radius or discontinuous if this change is similar to a first order phase transition. Use of a single characteristics gyration radius R to describe the state of the system is the simplest single parameter approach, which should be suitable for describing the folding–unfolding transition in terms of the increase of R. Generally the unfolded system state can have more complicated structure that requires a description in terms of more than a single parameter, like the necklace structures of unfolded states in poor solvents.[17]

We start with the free energy of the polymer as a function of its size. Generally there are three different cases for the configuration of the monomers. In a highly charged state the energy minimum is realized when the charges are strongly separated from each other. The optimum configuration is then a fully aligned polymer with the size given by its length $R_{\max} \sim N l_0$ where l_0 defines the length of the monomer or the persistence length of the polymer chain (since many characteristic radii will occur in our analysis, we have collected the notations in Table I).

The state of the polymer is folded at room temperature and low charging. Under these conditions the polymer forms

a three-dimensional condensed state with low free volume inside. The gyration radius corresponds to the compact structure of the size about $R_{\min} \sim N^{1/3} l_0$.

The intermediate state occurs at radius R between upper and lower limits

$$R_{\min} \ll R \ll R_{\max}. \tag{2.2}$$

Only in this regime can statistical mechanics be applied to define the free energy and the equilibrium state of the molecule. In fact for small gyration radius the free energy depends strongly on the specifics of the polymer interaction in the folded state while for large radius the details of near neighbor interaction and angular dependence of the energy should be significant.

To describe the phase transition between the uncharged folded state and charged extended state it is enough to know the properties of the system in the intermediate state. If the transition is continuous the gyration radius will continuously change through the intermediate regime. Free energy can be computed as a function of the gyration radius in that intermediate regime and the minimum of free energy defines the equilibrium state of the molecule. On the other hand if free energy has a maximum at intermediate radius one would expect the presence of two quasi equilibrium states at low and high radius separated by a barrier.

We restrict our consideration to the low-temperature case where the uncharged polymer is folded and the coupling energy exceeds the thermal energy.

Consider the free energy of the system at given gyration radius R that satisfies the condition (2.2), following the Flory theory version suggested in Ref. 15. The free energy is defined from the distribution function that contains both a statistical part (entropy) and an energy related part.

The statistical part of the $P(R)$ contains random walk Gaussian factor

$$p_{\mathrm{rw}}(R) \propto R^2 \exp\left[-\frac{3}{2}\left(\frac{R}{R_0} \right)^2 \right], \tag{2.3}$$

where R_0 is the radius of gyration of a random coil, $R_0 = l_0 N^{1/2}$. (Many different length parameters are used in this work. They are all described in Table I.) The details of the shape dependence of the polymer energy caused by its stiffness and other effects of the short-range interaction of next neighboring monomers are ignored here. As discussed in the introduction these effects should not affect our qualitative study for sufficiently long polymer. In accordance with the Flory theory[12] the opportunity for different monomers to occupy the same volume $v_0 \sim l_0^3$ should be excluded. This lowers the probability of small gyration radius. If we continuously fill the volume R^3 by N monomers then the allowed fraction of volume for the second monomer is reduced by the presence of the first monomer by the factor

$$1 - \frac{v_0}{R^3}. \tag{2.4}$$

For the monomer number k the reduction factor can be expressed similarly to Eq. (2.4) as

$$1 - \frac{(k-1)v_0}{R^3}. \tag{2.5}$$

For N monomers the reduction of the excluded volume can be expressed as the product of all factors (2.4) from $k=1$ to $k=N$[15]

$$p_{\mathrm{eV}}(R) = \prod_{k=1}^{N} \left(1 - \frac{(k-1)v_0}{R^3} \right). \tag{2.6}$$

The Nth term in Eq. (2.6) approaches zero, when the radius R is so small that the system is always folded

$$R \sim v_0 N^{1/3} \sim R_{\min}. \tag{2.7}$$

In this regime the theory is not applicable as we discussed before. For the intermediate regime Eq. (2.2) all factors in Eq. (2.6) are close to unity and we can expand the product as

$$p_{\mathrm{eV}}(R) \approx \exp\left(-\sum_{k=1}^{N} \frac{(k-1)v_0}{R^3} \right) = \exp\left(-\frac{N(N-1)v_0}{2R^3} \right). \tag{2.8}$$

The contributions of random walks (2.3) and excluded volume (2.8) define the weight factor

$$p_{\mathrm{tot}}(R) \approx R^2 \exp\left(-\frac{N(N-1)v_0}{2R^3} - \frac{3}{2}\left(\frac{R}{R_0} \right)^2 \right). \tag{2.9}$$

The distribution (2.9) describes the high-temperature regime, and the maximum of (2.9) with respect to the gyration radius is realized, when $R \sim N^{3/5}$

$$R_\infty \approx \frac{1}{2^{1/5}} N^{3/5} (l_0^2 v_0)^{1/5}, \tag{2.10}$$

instead of $R \sim N^{1/2}$ for random walks ignoring self-intersection. For the intermediate regime we ignore the conformational factor suggested in Ref. 15 since it does not depend on the radius R.

For the low temperature case under consideration the energy related terms are significant. For the system with short-range interaction the attractive energy describes nearby monomers. For the intermediate regime the probability for two monomers to be located nearby and overlap are similar. Therefore, we can use the factor

$$n_p = z \frac{N(N-1)v_0}{2R^3},$$

to describe the average number of close monomer pairs. The factor z is responsible for the excess of the number of neighboring positions compared to direct overlap. Making the reasonable assumption that close pairs can be described by some characteristic attractive average energy-J one can write the short range interaction energy as[15]

$$E_s = -zJ \frac{N(N-1)v_0}{2R^3}. \tag{2.11}$$

We consider the limit $N \gg 1$ that permits us to ignore energy fluctuations. This is especially well justified for homopolymers. The polymer is assumed to be sufficiently long (much

longer than its persistence length) to pay the most attention to the interaction of monomers located very far from each other in the polymer chain.

The Boltzmann distribution of polymers over their sizes can be expressed using the weight factor (2.9) and the probability becomes

$$p_{\mathrm{tot}}(R)\approx R^2\exp\left(-\frac{N(N-1)v_0}{2R^3}(1-z\beta J)-\frac{3}{2}\left(\frac{R}{R_0}\right)^2\right), \tag{2.12}$$

$$\beta=\frac{1}{k_BT}.$$

As follows from Eq. (2.12) the phase of the polymer is defined by the relationship of the temperature and characteristic binding energy zJ. In the regime of high temperature

$$k_BT>zJ, \tag{2.13}$$

the entropy (excluded volume) term dominates and the polymer is in extended (unfolded) state. In the regime of interest corresponding to low temperature

$$k_BT<zJ, \tag{2.14}$$

the distribution reaches its maximum at the small radius R corresponding to the folded state. For the sake of simplicity one can describe that maximum by seeking for the minimum possible value of R. We consider $R>R_{\mathrm{min}}$ and the energy (2.11) taken at $R=R_{\mathrm{min}}$ gives the folded state energy.

Our model can be compared with the real folding transition that occurs near room temperature $k_BT\sim 0.025\,\mathrm{eV}$. Then the binding energy of a monomer pair can be estimated as

$$J\sim\frac{0.025}{z}\,\mathrm{eV}\sim 0.0025\ \mathrm{eV}. \tag{2.15}$$

As the ''experimental'' parameter one can use the molecular dynamics simulation data,[12] deduced for cytochrome c protein containing $N\sim 100$ monomers. According to these data the total binding energy caused by the short-range interaction is about 0.2 eV (each monomer participates in about two bindings). Then the energy per the single monomer pair can be estimated as 0.2/100 eV$\sim$0.002 eV. This number is close to the estimate (2.15) for the energy of single binding. Thus one can see that theory and molecular-dynamic simulations are consistent with each other.

An alternative situation occurs when the polymer is neutral but composed of charged monomers and the Coulomb interaction of appropriately located positive and negative charges leads to the formation of a compact configuration at low temperature. The reasonable expectation is that due to the long-range character of the Coulomb interaction the energy is defined by the typical form for the Coulomb energy

$$E=-\frac{q_0^2}{R}. \tag{2.16}$$

The charge q_0 describes the characteristic charge fluctuation for the finite domain of the polymer. It was demonstrated in Ref. 10 that even in the absence of charge correlations the interaction is attractive for the neutral system (each local charge q interacts with the total charge $-q$ in the neutral system) and the charge q_0 scales as $N^{1/2}$. Then the distribution over radii can be written as [see Eq. (2.12)]

$$p_{\mathrm{tot}}(R)\approx R^2\exp\left(-\frac{N(N-1)v_0}{2R^3}-\frac{3}{2}\left(\frac{R}{R_0}\right)^2+\beta\frac{q_0^2}{R}\right). \tag{2.17}$$

We restrict our consideration to the low-temperature case where the Coulomb attraction term dominates the excluded volume term in the exponent in Eq. (2.17) until the minimum radius is approached. Therefore, the excluded volume term can be neglected under this assumption.

Finally we consider the effect of the external charge incorporated in the experiment similar to Refs. 2 and 12. If the molecule has total charge Q one would expect (for the intermediate state) that the total energy for the long-range repulsive Coulomb interaction is defined by long distances and has the standard form

$$E_Q=\eta\frac{Q^2}{\epsilon R}. \tag{2.18}$$

The Coulomb interaction strength is defined by long distances, since the interaction at distance R is defined by the total charge in the volume $Q_R\sim R^d$ (d is the system dimensionality) divided by the characteristic separation R. It scales as R^{d-1}, and therefore, the interaction is maximum at large R excluding one-dimensional case. The dielectric constant of the material is denoted ϵ and η is a constant coming from the geometry. This data can be compared to the molecular-dynamics simulations of Ref. 12, where the Coulomb energy for 19 electronic charges at the gyration radius $R\sim 3.5\,\mathrm{nm}$ has been estimated as 0.6 eV. In order to reproduce the estimated 0.6 eV, the ratio of dielectric constant to the geometric factor should be about 100. Since normally the geometric factor η is estimated to be around 1, the dielectric constant has to be very large ($\sim$100). The reason for this unreasonably large dielectric constant value is that in this crude model, the charge Q is taken as integer $+1$, no fraction charges exist. As a consequence, there is no delocalization of charge in the model, and the very important effects in charge-induced protein unfolding such as charge solvation have been totally ignored. In this regard, this model gives mostly qualitative description and cannot account for the detailed microscopic behaviors of the system.

Making use of the definition of the Coulomb energy of the external charge (2.18) one can write the distribution of the gyration radii for two cases of interest in the low-temperature limit. For the case of short-range interaction of monomers and the net Coulomb charge Q the distribution reads [see Eq. (2.12)]

$$\Omega_{\mathrm{sr}}(R)\approx R^2\exp\left(\frac{N(N-1)v_0}{2R^3}z\beta J-\frac{3}{2}\left(\frac{R}{R_0}\right)^2-\beta\eta\frac{Q^2}{\epsilon R}\right). \tag{2.19}$$

We neglected the contribution of the excluded volume since it has the same functional form as the attractive interaction but smaller due to the low temperature. Therefore it can be omitted.

For the long-range attraction of charged monomers as dominating interaction we get [see Eq. (2.17)]

$$\Omega_{\rm lr}(R)\approx R^2\exp\left(-\frac{N(N-1)v_0}{2R^3}-\frac{3}{2}\left(\frac{R}{R_0}\right)^2+\beta\left(\frac{q_0^2}{R}-\frac{\eta Q^2}{\epsilon R}\right)\right). \tag{2.20}$$

Here we keep the excluded volume term since it has different distance dependence compare to the Coulomb interaction energy. Therefore, they can be both significant for different gyration radii.

It is more convenient to describe the properties of the polymer in terms of the distribution logarithms defining the free energy $F=-k_BT\ln(\Omega)$. Then free energies for the short-range and long-range regimes can be written as

$$F_{\rm sr}(R)=-\frac{N(N-1)v_0}{2R^3}zJ+\frac{3}{2}k_BT\left(\frac{R}{R_0}\right)^2+\eta\frac{Q^2}{\epsilon R} \tag{2.21}$$

and

$$F_{\rm lr}(R)=k_BT\frac{N(N-1)v_0}{2R^3}+\frac{3}{2}k_BT\left(\frac{R}{R_0}\right)^2-\frac{q_0^2}{R}+\eta\frac{Q^2}{\epsilon R}. \tag{2.22}$$

Recall that the gyration radius is constrained from the lower side by $R_{\rm min}$. The preexponential term in Eqs. (2.19), (2.20) is omitted since it is always less important than the terms in the exponent. We will analyze the dependence of the gyration radius on the external charge in the next section.

III. ANALYTICAL STUDY OF CHARGING EFFECT ON THE POLYMER SIZE

A. Strong short-range interaction

We start by considering the polymer with short-range interaction between monomers. This polymer is described by the free energy (2.21). The equilibrium values of the gyration radius are defined by the free energy minima, either where the derivative of the expression (2.21) is zero or at the edge constraint radius $R_{\rm min}$

$$\frac{dF_{\rm sr}(R)}{dR}=\frac{3N(N-1)v_0}{2R^4}zJ+3k_BT\frac{R}{R_0^2}-\eta\frac{Q^2}{\epsilon R^2}=0. \tag{3.1}$$

We start with the analysis of the possible free energy minima within the folding regime $R=R_{\rm min}$. If the derivative (3.1) is negative at $R=R_{\rm min}$ then the free energy must have a minimum there. The second term on the right-hand side of Eq. (3.1) can be neglected in comparison with the first term near $R\sim R_{\rm min}$ at low temperature. In fact if we take $R_{\rm min}\sim l_0N^{1/3}$, $v_0\sim l_0^3$, $R_0\sim l_0N^{1/2}$ the ratio of first and second terms for $R\sim R_{\rm min}$ can be expressed as

$$\frac{zJ}{k_BT}N^{4/3}\gg 1,$$

because of the condition (2.14) for low temperatures and a large number of monomers $N\gg 1$.

Comparing two significant terms describing the short range and Coulomb energies we find that the free energy derivative is positive at $R=R_{\rm min}$, until the Coulomb repulsion energy at $R_{\rm min}$ would exceed three times the short-range attractive energy

$$3\frac{N(N-1)v_0}{2R_{\rm min}^3}zJ<\eta\frac{Q^2}{\epsilon R_{\rm min}}. \tag{3.2}$$

When the condition (3.2) is satisfied the folded state corresponds to a free energy maximum and it is not the stable state. The energy minimum occurs at large $R=R_{\rm ext}$ where the attractive energy can be neglected. Then solving Eq. (3.1) we find

$$R_{\rm ext}=R_0\left(\frac{\eta Q^2}{\epsilon R_0 3k_BT}\right)^{1/3}. \tag{3.3}$$

This radius is expected to be larger than the random walk radius R_0 because of the condition (3.2) (when that inequality is first satisfied we have $R_{\rm ext}\sim R_0N^{1/3}$).

When the total charge is small enough to satisfy the inequality opposite to Eq. (3.2)

$$3E_{\rm sh}>E_C,$$

$$E_{\rm sh}=\frac{N(N-1)v_0}{2R_{\rm min}^3}zJ, \tag{3.4}$$

$$E_C=\eta\frac{Q^2}{\epsilon R_{\rm min}}.$$

The free energy has its minimum at $R=R_{\rm min}$ so that the folded state is either stable or metastable. Equation (3.1) can have either zero or two solutions at $R>R_{\rm min}$. Exact algebraic analysis of the free energy second derivative shows that no solution exists at very small external charge

$$E_C<1.14E_{\rm sh}\left(\frac{R_{\rm min}}{R_0}\right)^{4/5}\left(\frac{k_BT}{E_{\rm sh}}\right)^{3/5} \tag{3.5}$$

the free energy has only one minimum at $R\sim R_{\rm min}$. When the Coulomb energy increase due to the charge is larger

$$E_C>1.14E_{\rm sh}\left(\frac{R_{\rm min}}{R_0}\right)^{4/5}\left(\frac{k_BT}{E_{\rm sh}}\right)^{3/5}, \tag{3.6}$$

Eq. (3.1) has two solutions. One solution can be very well approximated by $R_{\rm ext}$ [Eq. (3.3)] since the short-range interaction is not significant at long distances when the condition (3.6) is satisfied. This solution corresponds to the minimum of the free energy. The second solution is located between $R_{\rm min}$ and $R_{\rm ext}$. It describes the maximum of the free energy that must exist between two minima. The position of maximum can be found from Eq. (3.1) if we neglect the intermediate term [the consistency of this approach results from the condition (3.6)]. Solving Eq. (3.1) in this situation, we find

$$R\sim R_m\approx R_{\rm min}\left(\frac{3E_{\rm sh}}{E_C}\right)^{1/2}. \tag{3.7}$$

Thus one can specify three different regimes for the gyration radius behavior depending on the absolute value of charge. At very low charge Eq. (3.5) the system has only one stable state (free energy minimum, see Fig. 1) at $R=R_{\rm min}$. When the charge increases above the critical value given by

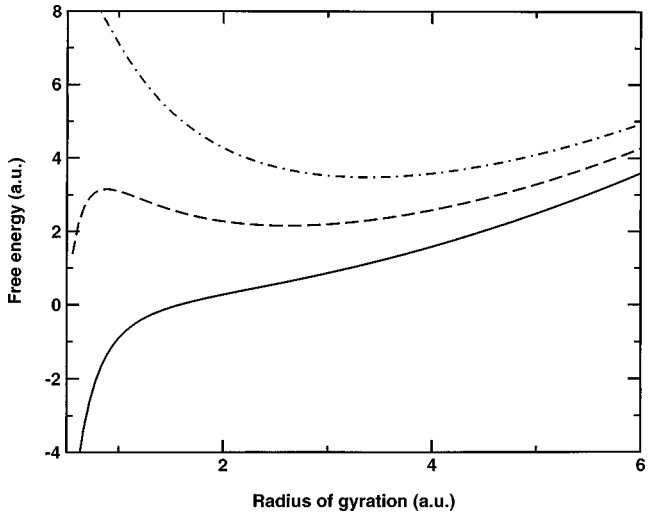

FIG. 1. The free energy as a function of radius of gyration at different charge Q. Note the plot here is only for illustration. The low charge regime is shown by the solid line. The charge regime, where the two states coexist is shown by the dashed line. The high charge regime where only the unfolded state is stable is shown by the dot–dashed line. We set $R_{\min}=0.5$ (see Table I).

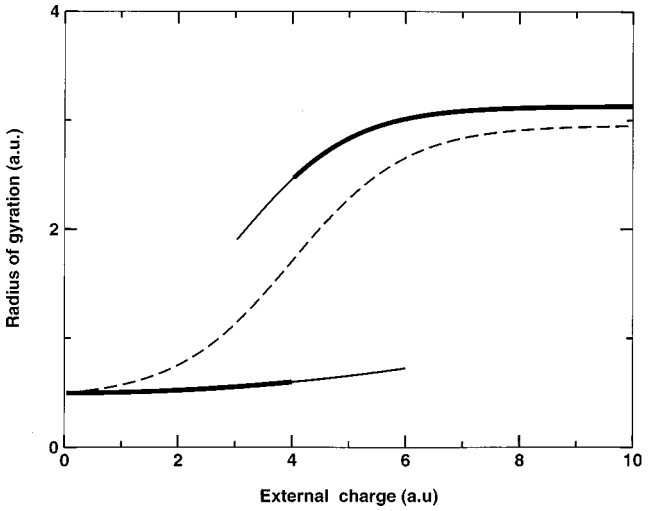

FIG. 2. The schematic dependence of gyration radius on the external charge. The solid line describes the polymer with short-range interaction of monomers and the dashed line describes the case of long-range interaction. Thick solid line shows the stable state, while thin solid line is for the metastable state.

Eq. (3.5) but below the second value given by the inequality (3.4) there are two free energy minima. One minimum exists at the gyration radius almost equal $R_{\min}$ while the second minimum occurs at a size exceeding the random walk range R_0. Therefore, those two sizes strongly differ from each other. They form possible equilibrium states of molecules separated by an energy barrier (see Fig. 1). The free energy stable state is defined by the deeper energy minimum. This minimum occurs at the small radius approximately when the Coulomb energy at $R_{\min}$ is less than the short-range energy

$$|E_{\mathrm{sh}}|>|E_C|, \tag{3.8}$$

or at large radius otherwise. Thus the radius of the thermal equilibrium stable polymer jumps from $R_{\min}$ to R_{ext}, when energies E_{sr} and E_C become equal. The dependence of the gyration radius on the external charge is shown schematically in Fig. 2. The change of the gyration radius is discontinuous similar to a first-order phase transition. Finally at very large charge, when $3E_{\mathrm{sr}}<E_C$ the small radius minimum of free energy vanishes and the folded state becomes absolutely unstable (Fig. 1).

Comparing the predictions of theory with the simulations data and experiment,[12] performed at room temperature one should consider two significant crossovers. These occur following the failure of Eq. (3.4), where the folded state becomes completely unstable and Eq. (3.8), where the folded state becomes metastable while the unfolded state is more stable. Our theory is not sufficiently accurate to estimate the crossover charges, although the experimental scale $Q\sim 10e$ is reasonable with our choice of parameters according to our discussion in the previous section. However, the difference by the factor $3^{1/2}$ between the charge satisfying the metastability criterion Q_m (3.8) and the charge Q_u, where the folded state becomes completely unstable can be used to interpret the results of Ref. 12. In fact, the experimental study shows unfolding at the external charge $10e$, while in the numerical simulations it occurs much later at $Q>17e$. The difference of 1.7 close to $3^{1/2}$ can occur due to the presence of two minima of the free energy in the range $10e<Q<17e$ with the lower minimum corresponding to unfolded state. Molecular dynamics simulations are started from the folded state. Since at $10e<Q<17e$ this state is metastable the transition to the lower unfolded state requires the system to overcome the energy barrier. The time of molecular-dynamics simulations is not long enough to describe the thermal activation of the cytochrome molecule. The experiments take longer time and the barrier between two minima is not high enough to keep the protein in the folded state. Therefore, the measured gyration radius exceeds the numerical predictions for that intermediate charge.

The increase of the molecular charge from $9e$ to $11e$ leads to jump like increase of the scattering cross section in agreement with our arguments. Perhaps at $Q\sim 10e$ the barrier separating two minima takes its highest value and experiment shows the presence of both folded and unfolded realizations of cytochrome since some molecules do not have enough time to unfold. We do not consider the temperature-induced folding–unfolding transition of uncharged or weakly charged protein. This transition can also be discontinuous[16] due to the interplay of the local chain stiffness and any interactions of far separated monomers. In our case the temperature is low enough to hold the uncharged system in a nearly collapsed state and the transition is driven by the Coulomb repulsion of external charges that is in competition with the short-range attraction responsible for the folded state.

The free energy expression (2.21) permits us to describe the characteristic average gyration radius as well as its fluctuations. Straightforward analysis shows that these fluctuations are small for the folded state due to the low temperature until it becomes completely unstable,

$$\Delta R\ll R_{\min}, \tag{3.9}$$

while in the unfolded state they can be described by the length scale of random walk

$$\Delta R \sim R_0. \tag{3.10}$$

In the experiments[2,12] the fluctuations of the scattering cross section are definitely larger for the unfolded state. The direct comparison of absolute values is not possible since for the unfolded state $R > R_0$ and the molecule can be almost transparent.

Our conclusions about the phase transition between folded and unfolded states caused by the excess charge in the case of short-range interaction agrees qualitatively with the numerical study of two state model later in this paper.

B. Molecule with long-range interaction of charged monomers

The polymer composed of charged monomers can be studied similarly to the previous subsection but with the different expression for the free energy Eq. (2.22). We are looking for the free energy minimum defined either by the derivative of the free

$$\frac{dF_{lr}(R)}{dR} = -3k_BT\frac{N(N-1)v_0}{2R^4} + 3k_BT\frac{R}{R_0^2} + \frac{1}{R^2}\left(q_0^2 - \eta\frac{Q^2}{\epsilon}\right) = 0, \tag{3.11}$$

energy or by the constraint radius $R_{\min}$. Two different regimes can be distinguished depending on the value of the external charge. When the external charge is low

$$Q < q_0\sqrt{\frac{\epsilon}{\eta}}, \tag{3.12}$$

the attractive interaction dominates. In this regime we can neglect the second (random walk) term in Eq. (3.11) since the equilibrium gyration radius is small in comparison with the high temperature equilibrium value Eq. (2.9)

$$R < R_\infty. \tag{3.13}$$

Then Eq. (3.11) can be solved and we get

$$R_1 = \sqrt{\frac{3}{2}\frac{k_BTN(N-1)v_0}{\left(q_0^2 - \eta\frac{Q^2}{\epsilon}\right)}}. \tag{3.14}$$

The minimum of free energy occurs at the larger of the solutions (3.14) or $R_{\min}$. Thus increase of the external charge to its crossover value given by Eq. (3.12) leads to continuous increase of the gyration radius until it reaches its infinite temperature value Eq. (2.10) (see Fig. 2).

When the external charge is sufficiently large to make the interaction repulsive on average

$$Q > q_0\sqrt{\frac{\epsilon}{\eta}}, \tag{3.15}$$

the radius keeps increasing and we should consider the effect of the repulsive and random walk term. A regime similar to Eq. (3.3) is then realized and the gyration radius takes the similar form

$$R_{l1} = R_0\left(\left(\eta\frac{Q^2}{\epsilon} - q_0^2\right)\frac{1}{R_0 3k_BT}\right)^{1/3}. \tag{3.16}$$

This regime is valid when the difference of charge terms is not too small so that $R_{l1} > R_\infty$. When the difference is small the effective interaction vanishes and the gyration radius is as in the high-temperature limit.

The behavior of the gyration radius for the charged monomers case is shown in Fig. 2 by the dashed line. Thus the gyration radius changes continuously with the external charge. The chain model simulations in Sec. IV for the polymer composed by charged monomers support this conclusion.

Thus we have considered two different models of a polymer: The first contains neutral monomers with short-range interactions and the second contains charged monomers with long-range Coulomb interactions in the low-temperature regime where the uncharged state is folded. The external charging leads to an unfolding transition. It is discontinuous in the case of the short-range interaction and continuous for the long-range interaction (see Fig. 2).

IV. LATTICE MODEL SIMULATIONS

The predictions of analytical theory (Secs. II and III) are made using the simple mean-field model most suitable for the intermediate radius state of the homopolymer. This model does not treat adequately most folded and most extended states.

In this section we are going to use the lattice model (see, e.g., Refs. 18–20), where the spatial polymer states are discretized. Monomers are treated as the points on a square lattice of the spacing a and the angles between subsequent directions from monomer to monomer are restricted to 90° or 180°.

The free energy, and especially entropy of polymers can be examined exactly by computer calculations on such lattice models if the number of sites (monomers) is not very large. The discretization of conformational space makes adequate sampling possible. To avoid computational pitfalls, an exhaustive enumeration of all conformations is performed to calculate exactly the partition function and thermal averages. Current computational power and the immensity of configuration space restrict our calculation to a chain of 12 monomers on the cubic lattice. Although the number of monomers is much less than that in any realistic polymer or protein, the total length of the polymer is larger than the persistence length that is about one to two lattice periods. Therefore we can expect a qualitatively reasonable estimate of the charging effect using exact thermal averaging.

Certainly this model is quite different from that studied in the first part of this work. It incorporates several features of real folded proteins including the specificity of interactions and the finite monomer size. The mean-field theory and the lattice model approach real polymer thermodynamics from different directions. Qualitative agreement between the predictions of these two approaches suggests that the main features of charging effects have been captured.

The goal of the computer work is to study the properties of the chain as a function of its net charge Q, temperature T

and interaction potential E, and compare the results with the predictions from the statistical theory of Secs. II, III, and with the experimental study.[12] As the oversimplified mean-field theory of Secs. II and III considers only the mean force of interaction, it cannot deal with fluctuations in interactions. Different potentials for the short-range monomer interaction instead of the homogeneous picture interactions used in the analytical theory can be used within the lattice model. The purpose of using different potentials in the simulations is to examine the sensitivity of the results to the fluctuations, and whether or not the physical picture emerging from the theory depends on the details of the potential.

Each monomer is assigned charge $+q_0$ or $-q_0$ ($q_0=1$ in our studies). The neutral chain is chosen to have alternating-charge monomers. The net charge of the chain is increased by flipping the -1 charge of one monomer to $+1$. Since there is more than one way to choose the beads to flip, all the possible choices, i.e., all the possible charge permutations are considered for each charge. The possible total excess charge for the 12-mer chain is $+2$, $+4$, $+6$, $+8$, $+10$, and $+12$. The results do not change qualitatively if the monomers are charged randomly.

The potential we use here is

$$E=\sum_{i\_j}\frac{q_iq_j}{r_{ij}}+\sum_{i\_j}B_{ij}\Delta(i,j). \tag{4.1}$$

The first term is the electrostatic potential and the second term accounts for the short-range interaction. $\Delta(i,j)=1$ if monomers i and j are separated by one lattice spacing but not connected by a bond (i.e., a so-called contact is formed), and zero otherwise. B_{ij} is a parameter that depends on the types of monomers i and j, and is defined by a specific potential.

To provide short-range interaction in the model close to the real system we will use two sorts of potentials [constants B in Eq. (4.1)]. The simplest type is the HP potential in which there are two types of monomers: hydrophobic (H) and polar (P); and B_{ij} is set to be unity only if both i and j are hydrophobic.[21] A more sophisticated pairwise potential has been suggested by Miyazawa and Jernigan (MJ potential) in which B_{ij} are the matrix elements of pairwise interactions of 20 amino acids.[22] In our calculations the MJ parameters are scaled by a factor of 0.2, in order to be compatible with the order of magnitude of the electrostatic energy. These interactions are more realistic than the constant interaction employed in the analytical study.

Our calculations consist of three steps: (a) generating lists of all spatial conformations and charge permutations; (b) using the lists to calculate various thermodynamic quantities for different potentials; (c) averaging the results over charge permutations according to Boltzmann weighing. The first monomer is located at the origin and the second one is fixed at (1,0,0) to eliminate the degeneracy related to rotation around the direction of the initial step. Except for the straight chain, all configurations have degeneracy due to reflection in the $x-y$ plane and $y-z$ plane, and symmetry under interchange of y and z axes. The total number of configurations for a 12mer chain, after removing all the degeneracy, is 881 147.

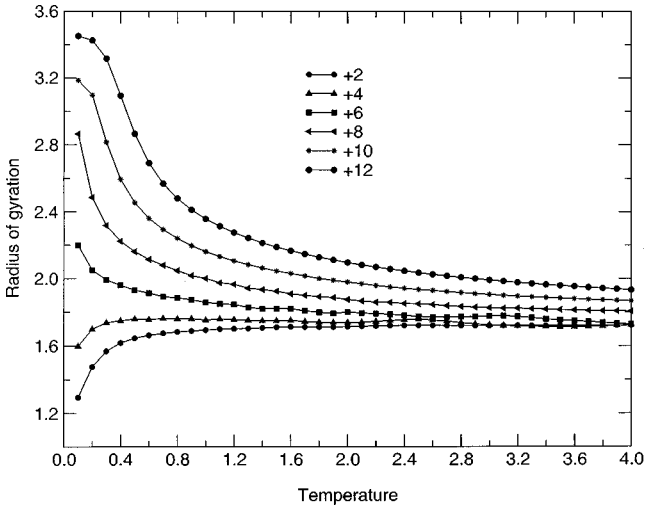

FIG. 3. The computed radius of gyration (expressed in units of lattice periods a) as a function of charge and temperature (in units of $0.1q_0^2/a$) in the case $B_{ij}=0$.

A property of interest, X, is written as a function of coordinates r and charge q, and its average is computed by averaging all the configuration space and charge permutation space.

$$\langle X(r,q)\rangle=\frac{\Sigma X(r,q)\exp(-E(r,q)/T)}{\Sigma\exp(-E(r,q)/T)}. \tag{4.2}$$

One result of our enumerations for a given set of interactions is the radius of gyration, the measure of the size of the chain, given by the mean-square deviation of the monomer coordinates from their inertia center. Its thermal average is computed as a function of charge and temperature.

First consider the case of absence of short-range interactions [B_{ij} is set to be 0 in Eq. (4.2)]. The radius of gyration is plotted as the function of charge and temperature (Fig. 3). The lowest temperature and the temperature interval are chosen to be $0.1q_0^2/a$. Even at low temperature $T\sim 0.1-0.5$, (''low'' in the sense that the low charge configurations stay compact), there is a continuous increase in radius of gyration as a function of charge that suggests a second-order transition from the compact to extended states, as predicted from the theory of the Sec. III B.

We have considered analytically (Secs. II and III) the low-temperature behavior only, while the simulations reveal the behaviors at various temperatures. There are two different behaviors in the temperature dependence of radius of gyration. For $Q\leqslant 4$, the radius of gyration increases significantly at first then slowly as a function of temperature. For $Q>4$, the radius of gyration decreases dramatically at first then slowly as a function of temperature. The reason is that for the low charges, the compact configurations are low-energy states and the extended ones are high-energy states; high temperature enables the chain to occupy the high-energy states, which leads to the increase in the average radius of gyration. For the high charges the reverse is true due to dominance of charge-charge repulsion. The dividing line of charge between these two types of behavior depends on the potential, but qualitatively the generality of two different

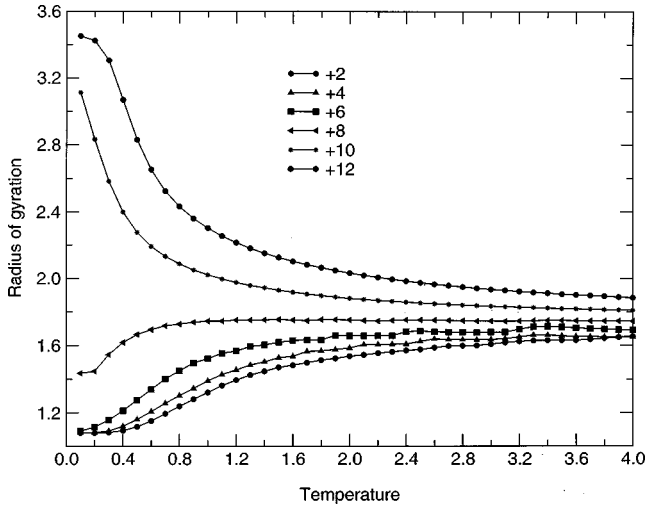

FIG. 4. The computed radius of gyration (in lattice periods a) as a function of charge and temperature (in the unit of $0.1q_0^2/a$) in the case $B_{ij}=-1$.

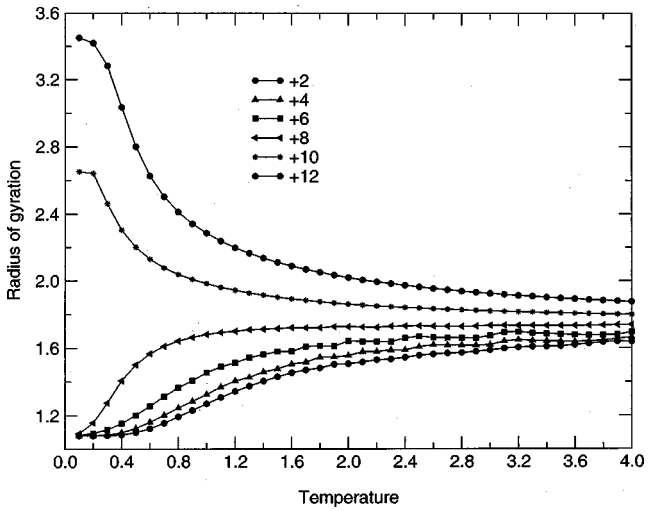

FIG. 5. The computed radius of gyration (in lattice periods a) as a function of charge and temperature (in units of $0.1q_0^2/a$) in the case of MJ potential as the short-ranged interactions.

temperature-dependent behaviors holds, as shown below. The distinction between these two different behaviors should not be taken as a sign for a first-order transition, since it has nothing to do with the discontinuity of populations of the states.

When the short-range interaction is turned on, the picture changes. Figure 4 shows the radius of gyration as a function of charge and temperature, when B_{ij} is set to be -1. It is a homopolymer model, and the degeneracy of the ground state is 73 (the same as the model without the short-range interactions). Overall the temperature-dependence of radius of gyration still has two types of behaviors as discussed above. Through all the temperatures the radii of gyration for $Q=2-6$ are similar. At low temperatures there is a significant jump in radius of gyration from $Q=8$ to $Q=10$. This is a signature of a first-order transition. Thus the gyration radius change with the external charge agrees with the expectation of the mean-field theory of Sec. III A.

If the model switches from homopolymer to heteropolymer, the nature of the transition does not change. To obtain a more realistic modeling description for the protein molecule, a sequence used in our calculations (PHE ILE CYS PHE CYS CYS ILE CYS MET CYS HIS PHE) is designed based on the MJ potential.[23] Examination of the density of states indicates that the degeneracy of the ground state is 1 as should be for the true folded state of the protein. The results from computer simulations are shown in Fig. 5. We see that there is still a first-order transition, a big jump in radius of gyration from $Q=8$ to $Q=10$ takes place at low temperatures. The critical charge Q_c at which the compact to extended transition occurs is larger, compared to Fig. 4, presumably due to the stronger short-range interactions in the MJ potential.

Figure 6 depicts the radius of gyration as a function of charge and temperature using the HP potential for B_{ij}. The HP sequence is $HHPHPHHPHPHH$ and it has a nondegenerate ground state. Interestingly, the first-order transition vanishes and the second-order transition occurs instead. The cooperativity (cooperativity refers to an all-or-none transition exhibited by proteins during folding) of HP sequences has been examined in the absence of electrostatic interactions, and it has been found that cooperativity is possessed by some sequences and is denied to others.[24] One possible reason for the HP potential destroying the first-order transition in Fig. 6 is that the discrimination against the contacts involving polar monomers breaks down the size dependence of the short-range interactions. In fact the theory of Sec. III is irrelevant for this case since the short-range interaction is repulsive.

To verify this, a modified HP potential is employed in which $B_{ij}=-1$ if i and j are both hydrophobic and $B_{ij}=-0.5$ otherwise. The modification is intended to keep the heterogeneous nature of HP sequence and enhance the size-dependence of the interactions. The results are depicted in Fig. 7. The first-order transition re-emerges, thus confirming that the heterogeneity of the short-range interactions does not affect the nature of the transition.

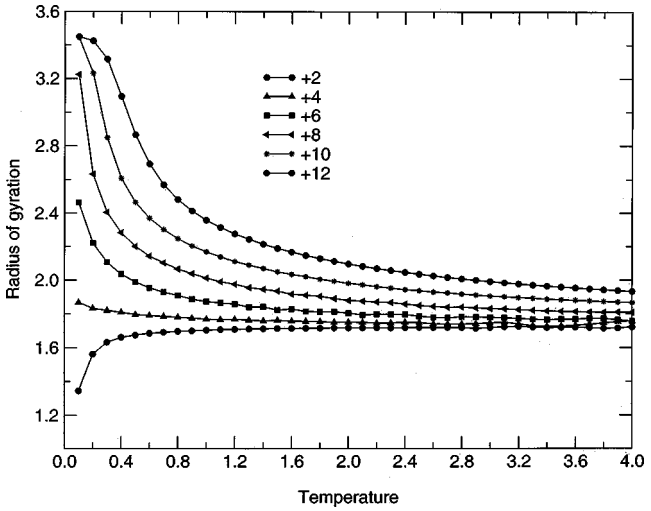

FIG. 6. The computed radius of gyration (in lattice periods a) as a function of charge and temperature (in units of $0.1q_0^2/a$) in the case of HP potential as the short-ranged interactions. The sequence is $HHPHPHHPHPHH$.

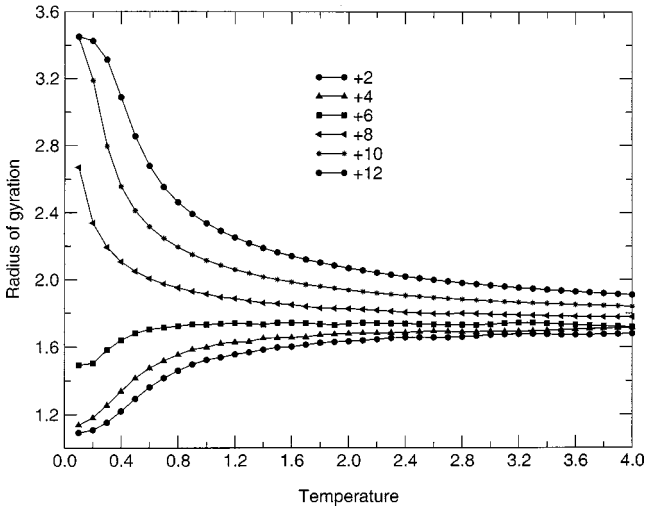

FIG. 7. The computed radius of gyration (in lattice periods a) as a function of charge and temperature (in the units of $0.1q_0^2/a$) with modified HP potential as the short-ranged interactions.

V. CONCLUSION AND DISCUSSION

In this paper we have studied the effect of the external charge on the size of a polymer molecule. Two different theoretical approaches have been suggested. The first approach is based on an analytical mean-field theory suitable for low temperatures and intermediate size of the molecule. The second approach uses lattice model simulations. Two different modeling systems have been considered, the polymer with a short-range interaction of monomers and polymer composed of charged monomers with a long-range Coulomb interaction. The first model is more realistic for the macromolecules like proteins while the second model is considered to show the opportunity of qualitatively different behavior.

Evident effect of charging at low temperature is the transition of molecule from the compact glob (folded) state of small size to the extended (unfolded) state of large size. This transition can be studied in the gas phase using a scattering cross section measurement technique,[2,12] and therefore, our results for the short-range model can be related directly to experiment.

The analytical approach enables us to describe the evolution of molecular size upon increasing the external charge incorporated into the molecule. We have found that the molecule with short-range interaction of monomers should undergo discontinuous transition from the compact to the extended state. In more detail two free energy minima separated by a barrier are formed by the interplay of short-range attractive and Coulomb repulsive interactions. The transition from a folded to an extended state occurs with the increase of charge as a jump between two those minima.

This conclusion is supported by the numerical analysis performed within the discrete lattice model of a polymer completed both for identical attraction of all monomers and for more realistic heteropolymer models with a degenerate ground state. Experimental study of Ref. 12 shows similar discontinuous behavior of the scattering cross section for the cytochrome c protein when the charge increases to more then 10 electronic charges. Moreover the analytical theory accounts for the discrepancy between the experimental and molecular dynamics study of Ref. 12. In fact the molecular dynamics predicts unfolding at the charge $17e$ (at room temperature) that differs from experimental value $10e$. This discrepancy can be explained by the analytical theory assuming that at charge $10e$ the folded state is metastable while at $17e$ it becomes completely unstable. Unfolding for the charge less than $17e$ requires overcoming an energy barrier. This process is too slow for molecular-dynamics simulations but can be sufficiently fast to proceed in the experiment. The ratio of upper and lower charges 17/10 agrees very well with the prediction of theory $3^{1/2}$.

To demonstrate the opportunity for the different transition scenarios we have examined a model with the long-range interaction of monomers. The size of the molecule increases continuously with charging in this model. The same conclusion can be drawn from the lattice model simulations.

One result of our enumeration of the lattice model for a given potential is the radius of gyration $R(Q,T)$, i.e., how the ensemble averaged radius of gyration changes as a function of charge and temperature. The low-temperature jump in radius of gyration as a function of charge is regarded as the signature of the first-order transition induced by charge. In general, we find strong qualitative agreement between simulation results and theoretical prediction. In the absence of short-range interaction, the compact-to-extended transition is of the second order; while in the presence of short-range interaction, the transition is of the first order. The details of the short-range interaction affect the value of Q for which the transition occurs, but certainly the nature of transition only depends on the coarse-grained description of a Hamiltonian, in this case whether or not the short-range interaction is present.

The mean-field analytical theory based on the homopolymer does not take into account the heterogeneity or fluctuations of the interactions, and simulations suggest that these approximations do not lead to disastrous effects in predicting the behavior of phase transition, and only the nature of the interactions (distance-dependence in this case) plays a crucial role.

Our finding that electrostatics only leads to a second-order transition and a combination of electrostatic and van der Waals interactions results in a first-order transition do not agree with previous lattice model studies on a very similar system. This was a three-dimensional lattice chain composed of random-charge monomers $\pm q_0$ with electrostatics only potential. There it was found that for longer chains "the radius is barely increasing for small Q, but an extreme steep rise begins beyond a threshold charge,[9]" the conclusion was not valid for chains as small as 13-mers. The disagreement may arise from the fact that the radius of gyration for longer chains was calculated by the Monte Carlo method, which has difficulties giving adequate sampling and the molecule tends to be trapped in some minimum. Consequently the size of the chain is overestimated at large Q and underestimated at small Q, so the slope of Q versus R near the transition is much sharper than it should be.

Cooperativity has been regarded as one of the very key

features of protein folding,[20,21] although its physical origin is not very well understood. The standard models so far do not involve electrostatics explicitly.[25–27] Our studies indicate that a charge (or *p*H) induced first-order transition is not particular to proteins. The heterogeneity of monomer–monomer interactions is not a prerequisite to the two-state behavior, so sequence has nothing to do with this type of cooperativity. Our findings suggest that in the electrostatically driven collapse or unfolding processes the behavior of proteins is not that different from that of other polymers. One direct implication of this is that the electrostatic force is not specific enough to be the dominant force in protein folding,[28] so that a more specific sequence-related force must play a vital role in determining the cooperative behavior that distinguishes proteins from other heteropolymers. The first-order transition found here arises from the interplay between the short-range and long-range interactions, which suggests that the key to protein's cooperativity may lie in how the native structure of proteins allows for the formation of contacts formed by residues distant in sequence. This suggestion echoes the findings from other lattice model studies on protein's cooperativity.[29]

ACKNOWLEDGMENTS

Funding from NIH, ARO, and The DOE/LBH Battery Program is acknowledged for partial support of this work.

[1] J. A. Schellman, Annu. Rev. Biophys. Biophys. Chem. **16**, 115 (1987).
[2] K. B. Shelimov, D. E. Clemmer, R. R. Hudgins, and M. F. Jarrold, J. Am. Chem. Soc. **119**, 2240 (1997); Y. Mao, J. Woenckhaus, J. Kolafa, M. A. Ratner, and M. F. Jarrold, *ibid.* **121**, 2712 (1999).
[3] Y. Takeoka, A. N. Berker, R. Du *et al.* Phys. Rev. Lett. **82**, 4863 (1999).
[4] K. Linderstrom-Lang, Compt. Rend. Trav. Lab. Carlsberg, Ser. Chim. **15**, 29 (1924).
[5] C. Tanford and J. G. Kirkwood, J. Am. Chem. Soc. **79**, 5333 (1957).
[6] A. Yang and B. Honig, J. Mol. Biol. **231**, 459 (1993).
[7] J. Antosiewitz, J. A. McCammon, and M. K. Gilson, J. Mol. Biol. **238**, 415 (1994).
[8] Macromolecules are finite systems and a phase transition does not exist in the rigorous sense. It is used here to refer to the two-state behavior in conformational change.
[9] Y. Kantor and M. Kardar, Phys. Rev. E **51**, 1299 (1995).
[10] Y. Kantor and M. Kardar, Phys. Rev. E **52**, 835 (1995).
[11] I. Velazquez, C. T. Reimann, and O. Tapia, J. Am. Chem. Soc. **121**, 11468 (1999).
[12] Y. Mao, M. A. Ratner, and M. F. Jarrold, J. Phys. Chem. B **103**, 10017 (1999).
[13] G. A. Arteca and O. Tapia, Int. J. Quantum Chem. **80**, 848 (2000).
[14] F. J. Solis and M. Olvera de la Cruz, Eur. Phys. J. E **4**, 143 (2001).
[15] J. D. Bryngelson and P. G. Wolynes, Biopolymers **30**, 177 (1990); P. J. Flory, *Principles of Polymer Chemistry* (Cornell University, Ithaca, 1953).
[16] C. B. Post and B. H. Zimm, Biopolymers **18**, 1487 (1979); A. Kolinski, J. Skolnick, and R. Yaris, J. Chem. Phys. **85**, 3585 (1986).
[17] P. Chodanowski and S. Stoll, J. Chem. Phys. **111**, 6069 (1999); A. V. Dobrynin, M. Rubinstein, and S. P. Obukhov, Macromolecules **29**, 2974 (1996).
[18] E. I. Shakhnovich, Curr. Opin. Struct. Biol. **7**, 29 (1997).
[19] V. S. Pande, A. Y. Grosberg, T. Tanaka, and D. S. Rokhsar, Curr. Opin. Struct. Biol. **8**, 68 (1998).
[20] E. I. Shakhnovich and A. V. Finkelstein, Biopolymers **28**, 1667 (1989).
[21] K. F. Lau and K. A. Dill, Macromolecules **22**, 3986 (1989).
[22] S. Miyazawa and R. L. Jernigan, Macromolecules **18**, 534 (1985).
[23] E. I. Shakhnovich and A. M. Gutin, Protein Eng. **177**, 793 (1993).
[24] H. S. Chan and K. A. Dill, Philos. Trans. R. Soc. London, Ser. B **348**, 61 (1995).
[25] K. A. Dill, K. M. Fiebig, and H. S. Chan, Proc. Natl. Acad. Sci. U.S.A. **90**, 1942 (1993).
[26] E. I. Shakhnovich and A. V. Finkelstein, Biopolymers **28**, 1667 (1989).
[27] A. Kolinski, W. Galazka, and J. Skolnick, Proteins **26**, 271 (1996).
[28] K. A. Dill, Biochemistry **29**, 7133 (1990).
[29] V. I. Abkevich, A. M. Gutin, and E. I. Shakhnovich, J. Mol. Biol. **252**, 460 (1995).